Implicit conservative upwind schemes for strongly transient flows

Gérard Fernandez

INRIA

UNITÉ DE RECHERCHE
INRIA-SOPHIA ANTIPOLIS

Institut National
de Recherche
en Informatique
et en Automatique

Domaine de Voluceau
Rocquencourt
B.P. 105
78153 Le Chesnay Cedex
France
Tél.: (1) 39 63 55 11

Rapports de Recherche

N° 873

IMPLICIT CONSERVATIVE UPWIND SCHEMES FOR STRONGLY TRANSIENT FLOWS

Gérard FERNANDEZ

JUILLET 1988

RR-0873

IMPLICIT CONSERVATIVE UPWIND SCHEMES FOR STRONGLY TRANSIENT FLOWS

Gérard Fernandez

INRIA
2004, Route des Lucioles
Sophia Antipolis 1 et 2
06560 VALBONNE FRANCE

Abstract

Numerical comparisons with several classical upwindings applied to the shock tube problem are presented. Implicit schemes are choosen for their linear unconditionally stability property. Attention is given to the large time steps which can be really used in this unsteady test problem. We are also interested in the behavior of the schemes used when applied to low Mach number flow calculations.

SCHEMAS CONSERVATIFS IMPLICITES ET DECENTRES POUR DES ECOULEMENTS FORTEMENT NON STATIONNAIRES

Gérard Fernandez

INRIA
2004, Route des Lucioles
Sophia Antipolis 1 et 2
06560 VALBONNE FRANCE

Résumé

Des comparaisons numériques de différentes techniques de décentrage appliquées au problème du tube à choc sont présentées dans ce rapport. Nous avons choisi les schémas implicites pour leur propriété de stabilité linéaire inconditionnelle et observons les limites des pas de temps qu'on peut réellement utiliser sans détériorer complètement la précision de la solution instationnaire du problème considéré. Nous étudions aussi le comportement de ces schémas dans un cas d' écoulement subsonique.

Contents

1 Introduction

In this paper we compare several implicit upwind conservative schemes applied to the classical shock tube problem. Numerous schemes have been presented for the numerical simulation of the Euler equations, and successfully applied in the steady case. We deal here with the implicit linearized schemes used by Beam and Warming [21], and present three kinds of implicit formulations. The first one is a first-order implicit linearized scheme, the second one is a modified Newton method, and the third one use partly second-order extensions.

The schemes used are linearly unconditionally stable, but we are also interested by nonlinear stability. Unfortunately, there are few theoretical investigations of this subject: Harten has shown that some implicit nonconservative upwind schemes are T.V.D [8]. As we want to investigate unsteady solutions with shock we prefer fully conservative schemes. That is the reason why we present several numerical experiments illustrating the behaviours of the schemes with a simple unsteady test case: the shock tube problem. First we use the same initial data than Sod in [12], two other initial data are chosen in order to obtain subsonic or supersonic velocities.

After recalling the governing equations in the the next section, we describe the numerical schemes in some details in the finite-element context. We choose a sample of some upwind numerical flux functions for the Euler equations, and build the implicit linearized version of the schemes from these flux functions. The selected upwind schemes (Steger-Warming, Vijayasundaram, Roe, van Leer, and Osher schemes) are first compared using their explicit version. Since a small time step is used (under CFL condition), the numerical results point out the accuracy obtained by the schemes by a comparison to the exact solution. The implicit formulations are then used with large time step on the same test problems in order to find the robustness limit and to know their behaviours. Using the numerical results we conclude this paper by choosing one of these schemes to investigate low Mach number reactive flows in forthcoming studies ([4]).

2 Equations

We consider the two-dimensional Euler equations:

$$W_t + \nabla.\mathbf{F}(W) = 0 \tag{1}$$

where

$$W = \begin{pmatrix} \rho \\ \rho u \\ \rho v \\ \rho E \end{pmatrix}, \ \mathbf{F}(W) = \begin{pmatrix} F_1 \\ F_2 \end{pmatrix}, \ F_1(W) = \begin{pmatrix} \rho u \\ \rho u^2 + p \\ \rho uv \\ (\rho E + p)u \end{pmatrix}, \ F_2(W) = \begin{pmatrix} \rho v \\ \rho uv \\ \rho v^2 + p \\ (\rho E + p)v \end{pmatrix}.$$

For an ideal gas with constant specific heats the state equation writes:

$$p = (\gamma - 1)\rho e \tag{2}$$

with

$$\rho E = \rho e + \frac{1}{2}\rho(u^2 + v^2)$$

ρ is the gas density, ρu and ρv the momentum components, ρE and ρe are respectively the total and internal energy per unit volume, p is the pressure and $\gamma = 1.4$ is the ratio of the specific heats for a diatomic gas.
We shall use the notation

$$F = \eta_1 F_1 + \eta_2 F_2 \tag{3}$$

and recall that system (1) is hyperbolic, since the Jacobian matrix

$$A(W) = \frac{\partial F(W)}{\partial W} \tag{4}$$

is diagonalisable and has real eigenvalues for all physically relevant values of $(\eta_1, \eta_2, W) \in I\!R \times I\!R \times I\!R^4$ (that is $\rho > 0$). The eigenvalues of A are the following:

$$\begin{cases} \lambda_1 = \lambda_2 = \eta_1 u + \eta_2 v \\ \lambda_3 = \lambda_1 + c(\eta_1^2 + \eta_2^2)^{\frac{1}{2}} \\ \lambda_4 = \lambda_1 - c(\eta_1^2 + \eta_2^2)^{\frac{1}{2}} \end{cases}$$

where c is the isentropic local sound speed defined by $c^2 = \gamma p/\rho$.
We also recall that the fluxes function (3) is homogeneous of degree 1. By using Euler's theorem this property writes:

$$F(W) = A(W)W \tag{5}$$

We shall use in the next sections the additional notations:

$$\begin{cases} A = T\Lambda T^{-1},\ \Lambda \text{ diagonal} : \Lambda = (\lambda_k)_{k=1,4}\ , \\ |A| = T|\Lambda|T^{-1},\ |\Lambda| = (|\lambda_k|)_{k=1,4}\ . \\ \Lambda + |\Lambda| = 2\Lambda^+,\ A^+ = T\Lambda^+T^{-1} \\ \Lambda - |\Lambda| = 2\Lambda^-,\ A^- = T\Lambda^-T^{-1} \end{cases}$$

where Λ is the eigenvalue matrix and T and T^{-1} the similarity transformation matrices defined by:

$$T(W) = \begin{pmatrix} 1 & 0 & \frac{1}{2c^2} & \frac{1}{2c^2} \\ u & \tilde{\eta}_2 & \frac{u + c\tilde{\eta}_1}{2c^2} & \frac{u - c\tilde{\eta}_1}{2c^2} \\ v & -\tilde{\eta}_1 & \frac{v + c\tilde{\eta}_2}{2c^2} & \frac{v - c\tilde{\eta}_2}{2c^2} \\ \frac{u^2+v^2}{2} & \tilde{\eta}_2 u - \tilde{\eta}_1 v & \frac{h + c(\tilde{\eta}_1 u + \tilde{\eta}_2 v)}{2c^2} & \frac{h - c(\tilde{\eta}_1 u + \tilde{\eta}_2 v)}{2c^2} \end{pmatrix}$$

$$T^{-1}(W) = \begin{pmatrix} 1 - \frac{\gamma-1}{c^2}\cdot\frac{u^2+v^2}{2} & \frac{\gamma-1}{c^2}u & \frac{\gamma-1}{c^2}v & -\frac{\gamma-1}{c^2} \\ \tilde{\eta}_1 v - \tilde{\eta}_2 u & \tilde{\eta}_2 & -\tilde{\eta}_1 & 0 \\ -c(\tilde{\eta}_1 u + \tilde{\eta}_2 v) + (\gamma-1)\frac{u^2+v^2}{2} & c\tilde{\eta}_1 - (\gamma-1)u & c\tilde{\eta}_2 - (\gamma-1)v & \gamma-1 \\ c(\tilde{\eta}_1 u + \tilde{\eta}_2 v) + (\gamma-1)\frac{u^2+v^2}{2} & -c\tilde{\eta}_1 - (\gamma-1)u & -c\tilde{\eta}_2 - (\gamma-1)v & \gamma-1 \end{pmatrix}$$

where $h = E + p/\rho$ is the enthalpy and

$$\tilde{\eta}_1 = \frac{\eta_1}{(\eta_1^2 + \eta_2^2)^{\frac{1}{2}}}\ ,\quad \tilde{\eta}_2 = \frac{\eta_2}{(\eta_1^2 + \eta_2^2)^{\frac{1}{2}}}\ .$$

3 Numerical schemes

3.1 F.E.M/F.V.M approach

We consider the flow in a bounded subdomain Ω of $I\!R^2$. In order to capture solutions with discontinuities (1) is rewritten in the integral form:

$$\frac{d}{dt}\int\int_{\Omega} W\,dxdy + \int_{\partial\Omega}(n_x F_1(W) + n_y F_2(W))d\sigma = 0 \qquad (6)$$

where $\overrightarrow{n} = (n_x, n_y)$ denotes the outward normal vector to $\partial\Omega$ which is the boundary of the domain Ω. The mixed finite-element/finite-volume method consists in using a finite-volume formulation with a standard finite-element triangulation. A cell is constructed around every vertex of the triangulation by means of the centroids G of the neighboring triangles. Figure A gives a description of a cell (control volume) which will be noted C_i for the vertex i.

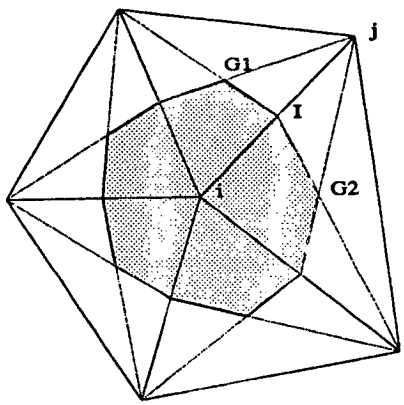

Figure A : Control volume C_i

The discrete equations are obtained by considering the form (6) on each cell C_i. By using a first-order accurate approximation for the temporal derivative, we get the first-order conservative explicit scheme:

$$\frac{W_i^{n+1} - W_i^n}{\Delta t} = -\frac{1}{area(C_i)}\sum_{j\in\mathcal{K}(i)}\Phi(W_i^n, W_j^n, \overrightarrow{\eta}_{ij}) \qquad (7)$$

where Φ is the numerical flux function, $\mathcal{K}(i)$ is the set of neighboring nodes of i, and the vector $\overrightarrow{\eta}_{ij} = (\eta_1, \eta_2)$ is computed by means of the outward unit normal vector $\overrightarrow{n}_{ij} = (n_{ij}^x, n_{ij}^y)$ on ∂C_i, with

$$\eta_1 = \int_{G_1 I G_2} n_{ij}^x d\sigma \;;\quad \eta_2 = \int_{G_1 I G_2} n_{ij}^y d\sigma \;.$$

The discrete flux function Φ is built directly from equation (3) on each bisegment (ij), which leads to a one dimensional formulation. (For the sake of simplicity we shall odmit η in the next notations and write the numerical fluxes as function of two arguments denoted W_L and W_R instead of W_i and W_j.)
Following Harten Lax and van Leer [9], we write the numerical flux function Φ in the general form, whether it be centered or not:

$$\Phi(W_L, W_R) = \frac{F(W_L) + F(W_R)}{2} - \frac{1}{2} d(W_L, W_R)$$

where $d(W_L, W_R)$ is some function which contains the numerical viscosity terms. The consistency requires that:

$$d(W, W) = 0$$

We refer to [2] for further details on the method and to [20,5] for its use with respectivelly first-order and second-order explicit upwind schemes.

3.2 Conservative upwind schemes

Most of the existing upwind schemes are based on the splitting of the Jacobian matrix A in its positive and negative parts, $A = A^+ + A^-$. We are first going to compare three conservative upwind centered schemes. They all belong to the family of Q-schemes ; following van Leer [16], we write them :

$$\Phi^Q(W_L, W_R) = \frac{F(W_L) + F(W_R)}{2} + Q(W_L, W_R)(W_L - W_R)$$

The flux formulas are given below :

- Vijayasundaram flux function [20]

$$\Phi^{VIJ}(W_L, W_R) = A^+(\frac{W_L + W_R}{2})W_L + A^-(\frac{W_L + W_R}{2})W_R$$

Setting $\tilde{B}(W_L, W_R) = \tilde{A}(W_L, (W_L + W_R)/2)$, Vijayasundaram Q-part writes:

$$Q^{VIJ} = \frac{1}{2}[\ |A(\frac{W_L + W_R}{2})| + \frac{1}{2}\tilde{B}(W_R, W_L) - \frac{1}{2}\tilde{B}(W_L, W_R)\ ]$$

- Harten van Leer flux function [9]

$$\Phi^{HVL} = \frac{F(W_L) + F(W_R)}{2} + \frac{1}{2}|A(\frac{W_L + W_R}{2})|(W_L - W_R)$$

- Roe flux function [11]

$$\Phi^{ROE} = \frac{F(W_L) + F(W_R)}{2} + \frac{1}{2}|\tilde{A}(W_L, W_R)|(W_L - W_R)$$

where $\tilde{A}$ is some matrix "close" to A and satisfies the following property:

$$\tilde{A}(W_L, W_R)(W_L - W_R) = F(W_L) - F(W_R) \tag{8}$$

For Euler equations such a matrix has been defined by Roe. The similarity transformation matrices (T, T^{-1}) and the eigenvalues matrix (Λ) are computed by means of the following averaged values:

$$\begin{cases} u = \dfrac{\sqrt{\rho_L}u_L + \sqrt{\rho_R}u_R}{\sqrt{\rho_L} + \sqrt{\rho_R}} \\ v = \dfrac{\sqrt{\rho_L}v_L + \sqrt{\rho_R}v_R}{\sqrt{\rho_L} + \sqrt{\rho_R}} \\ h = \dfrac{\sqrt{\rho_L}h_L + \sqrt{\rho_R}h_R}{\sqrt{\rho_L} + \sqrt{\rho_R}} \end{cases}$$

The sound speed being defined by

$$c^2 = (\gamma - 1)(h - \frac{1}{2}[u^2 + v^2])$$

the matrix $\tilde{A}$ is obtained by the relation $\tilde{A} = T\Lambda T^{-1}$. The average value of the density is not used since this variable does not appear in the eigenvalue matrix or in the similarity transformation matrices. Property (8) allows us to rewrite Roe scheme in the following simpler forms:

$$\Phi^{ROE}(W_L, W_R) = F(W_L) - \tilde{A}^-(W_L - W_R)$$

or

$$\Phi^{ROE}(W_L, W_R) = F(W_R) + \tilde{A}^+(W_L - W_R)$$

Moreover, the discretisation corresponds to a linearized Riemann problem on each bisegment ij. If W_L and W_R satisfy the shock condition:

$$F(W_L) - F(W_R) = \lambda(W_L - W_R)$$

then λ is an eigenvalue of $\tilde{A}(W_L, W_R)$ and $W_L - W_R$ is the associated eigenvector. The exact solution of the linearized Riemann problem is obtained.

In addition to these three Q-schemes we will also study the fully upwind scheme of Steger-Warming which writes :

- Steger-Warming flux function [13]

$$\Phi^{SW}(W_L, W_R) = A^+(W_L)W_L + A^-(W_R)W_R$$

Remark 1 : All these schemes are linearly equivalent up to the second order. Except for Steger-Warming scheme they remain nonlinearly equivalent up to the second order far from discontinuities.

Remark 2 : Except for Roe scheme and Steger-Warming scheme, these schemes are not fully upwind when all the eigenvalues have the same sign.

Remark 3 : Absolute values make these schemes nondifferentiable in the W_L, W_R variables.

We shall use two other numerical fluxes, Osher scheme and van Leer flux vector splitting that we define below :

- Osher flux function [10]

$$\Phi(W_L, W_R) = \frac{F(W_L) + F(W_R)}{2} - \frac{1}{2} d(W_L, W_R)$$

$$d(W_L, W_R) = \int_{W_L}^{W_R} |A(W)| \, dW$$

where the path integration is defined in the state space by means of the Riemann invariants.

- Van Leer flux function [19]

$$\Phi(W_L, W_R) = F^+(W_L) + F^-(W_R)$$

where $F^-(W) = F(W) - F^+(W)$ and F^+ is given in the one-dimensional case:

$$F^+(W) = \begin{cases} F & if \quad M \geq 1 \\ \left\{ \begin{array}{l} f_1^+ = \frac{\rho c}{4}(M+1)^2 \\ f_2^+ = \frac{f_1^+}{\gamma}((\gamma-1)u + 2c) \\ f_3^+ = f_1^+ [\frac{[(\gamma-1)u+2c]^2}{2(\gamma^2-1)}] \end{array} \right\} & if \quad |M| < 1 \\ 0 & if \quad M \leq -1 \end{cases}$$

where u is the velocity and $M = u/c$ is a local algebraic Mach number.
We refer to [19] and to [10] for a complete description of these two numerical flux functions, and to [6] and [7] for their use with finite-element method.

3.3 Implicit conservative schemes

• Implicit linearized scheme :

The main tools we use to built an implicit linearized non factored scheme are:

1/ A linearization of fluxes [21]:

After a first-order expansion of the Taylor series we write

$$\Phi(W_L^{n+1}, W_R^{n+1}) = \Phi(W_L^n, W_R^n) + \frac{\partial \Phi}{\partial W_L}(W_L^n, W_R^n)(W_L^{n+1} - W_L^n) + \frac{\partial \Phi}{\partial W_R}(W_L^n, W_R^n)(W_R^{n+1} - W_R^n)$$

2/ A simplification [15]:

When the explicit flux function can be written in the form

$$\Phi(W_L^n, W_R^n) = H_1(W_L^n, W_R^n) W_L^n + H_2(W_L^n, W_R^n) W_R^n \tag{9}$$

we use instead of the exact Jacobian matrix of Φ the matrices H_1 and H_2 :

$$\frac{\partial \Phi}{\partial W_L}(W_L^n, W_R^n) \simeq H_1(W_L^n, W_R^n) \quad , \quad \frac{\partial \Phi}{\partial W_R}(W_L^n, W_R^n) \simeq H_2(W_L^n, W_R^n) \tag{10}$$

Remark 4 : All the schemes described in the previous section, except perhaps the Osher flux, can be written in the form (9).

We shall use the simplified form for all cases where the Jacobian of Φ does not exist, so for the Q-schemes we get an implicit flux function similar to the explicit one:

$$\Phi^{n+1}(W_L, W_R) = H_1(W_L^n, W_R^n) W_L^{n+1} + H_2(W_L^n, W_R^n) W_R^{n+1}$$

where

$$H_1(W_L^n, W_R^n) = \frac{1}{2}[A(W_L^n) + Q(W_L^n, W_R^n)] \quad , \quad H_2(W_L^n, W_R^n) = \frac{1}{2}[A(W_R^n) - Q(W_L^n, W_R^n)]$$

With the finite-volume method the scheme writes:

$$\frac{W_i^{n+1} - W_i^n}{\Delta t} + \frac{1}{area(C_i)} \sum_{j \in \mathcal{K}(i)} \mathcal{A}_{ij}^n W_j^{n+1} = 0$$

where

$$\mathcal{A}_{ii}^n = \sum_{j \in \mathcal{K}(i)} H_1(W_i^n, W_j^n) \quad , \quad \mathcal{A}_{ij}^n = H_2(W_i^n, W_j^n) \quad .$$

With the notations N for the number of vertex and $\delta W^{n+1} = W^{n+1} - W^n \in I\!R^{4N}$, we recall the algorithm written as a two phase scheme in the "δ-formulation" :

- Physical or explicit phase:

$$\delta\hat{W} = \Delta t \mathcal{F}(W^n)$$

- Mathematical or implicit phase:

$$[I\!I + \Delta t \mathcal{A}(W^n)]\delta W^{n+1} = -\delta\hat{W}$$

Where $\mathcal{F}(W^n) \in I\!R^{4N}$ is some explicit approximation of the first or second-order accuracy (described in a following section) of the explicit fluxes, the i-th component writes:

$$\mathcal{F}_i(W) = \sum_{j \in \mathcal{K}(i)} \Phi(W_i^n, W_j^n, \vec{\eta}_{ij})$$

By using (10) the linear operator $\mathcal{A}$ rewrites:

$$\mathcal{A}_{ij} \simeq \frac{\partial \mathcal{F}_i(W)}{\partial W_j}$$

The identity operator $I\!I$ comes from the temporal derivative.

Remark 5 : We can use different flux functions in the two phases, for instance, the Steger-Warming flux function in the implicit phase with the Osher flux in the explicit phases.
When the true Jacobian is used the method can be viewed as a Newton-like method for steady solution when Δt is arbitrarily large.

- **Non linear implicit scheme :**

At each time step the previous method might be interpreted as the first iteration of a Newton like method to search the zero of the functional $G(X)$:

$$G(X) = X - W^n + \Delta t \mathcal{F}(X) \ .$$

By applying Newton algorithm

$$G'(X^\alpha)(X^{\alpha+1} - X^\alpha) = -G(X^\alpha)$$

with

$$G'(X^\alpha) = [I\!I + \Delta t \mathcal{A}(X^\alpha)]$$

the linearized implicit scheme is obtained by the first iteration with W^n for X^0.
We derive another version by pursueing the iterative process until we get a residue

$|X^{\alpha+1} - X^{\alpha}|$ small enough.
The algorithm is written in two phases that are applied iteratively till convergence:

- phase 1:

$$\delta\hat{W}^{\alpha} = (W^{\alpha} - W^{n}) + \Delta t\mathcal{F}(W^{\alpha})$$

- phase 2:

$$[I\!I + \Delta t\mathcal{A}(W^{\alpha})]\delta W^{\alpha+1} = -\delta\hat{W}^{\alpha}$$

Since we use upwind schemes,the linear systems obtained by linearization are well conditionned for Gauss-Seidel relaxation algorithm. We refer to [14,15] for stability and convergence results.

3.4 Second-order extensions

Second-order accurate explicit schemes in both space and time are obtained by following the M.U.S.C.L method introduced by B. van Leer [17] for the spatial approximation, and a predictor/corrector sequence for the temporal approximation. Partly second-order extensions of the previous implicit schemes are obtained by introducing in the "δ-formulation" a spatial second-order explicit phase and a three level time integration.
In order to avoid oscillations some local "limiting process" are applied to return to first-order accuracy when it is necessary. The variables (ρ, u, v, p) are well adapted to that limiting process and procure some extra robustness for the schemes.

- **Spatial scheme :**

Using standard P-1 Galerkin interpolant for $\tilde{W} = (\rho, u, v, p)$ on each triangle, an approximate gradient of $\tilde{W}$ at the vertex i is constructed as:

$$\begin{cases} \tilde{W}_x(i) = \dfrac{1}{area[supp(i)]} \displaystyle\int\int_{supp\ (i)} \frac{\partial \tilde{W}}{\partial x}\, dxdy\ , \\ \tilde{W}_y(i) = \dfrac{1}{area[supp(i)]} \displaystyle\int\int_{supp\ (i)} \frac{\partial \tilde{W}}{\partial y}\, dxdy\ , \end{cases} \tag{11}$$

Where $supp\ (i)$ is the set of triangles having i as a vertex ; $\tilde{W}_{ij}$ and $\tilde{W}_{ji}$ are then defined by:

$$\begin{cases} \tilde{W}_{ij} = \tilde{W}_i + \frac{1}{2}\begin{pmatrix} \tilde{W}_x(i) \\ \tilde{W}_y(i) \end{pmatrix} . \overrightarrow{ij} \\ \tilde{W}_{ji} = \tilde{W}_j + \frac{1}{2}\begin{pmatrix} \tilde{W}_x(j) \\ \tilde{W}_y(j) \end{pmatrix} . \overrightarrow{ji} \end{cases} \tag{12}$$

Going back to conservative variables, second-order accurate approximation of the fluxes on every bisegment ij is then given by the expression:

$$\Phi_{ij} = \Phi(W_{ij}, W_{ji}) \tag{13}$$

Where Φ is one of the numerical flux functions previously defined.

- **Explicit scheme :**

A very cheap procedure is obtained by using in both predictor step and corrector step the approximate gradient (11).

◇ The predictor step is centered and linearized:

$$\tilde{W}_i^* = \tilde{W}_i^n - \frac{\Delta t}{2}[\frac{\partial F_1(\tilde{W}_i)}{\partial \tilde{W}_i}\tilde{W}_x(i) + \frac{\partial F_2(\tilde{W}_i)}{\partial \tilde{W}_i}\tilde{W}_y(i)] \tag{14}$$

◇ The corrector step is the following:

$$\begin{cases} \tilde{W}_{ij} = \tilde{W}_i^* + \frac{1}{2}\begin{pmatrix}\tilde{W}_x(i)\\ \tilde{W}_y(i)\end{pmatrix}.\overrightarrow{ij} \\ \tilde{W}_{ji} = \tilde{W}_j^* + \frac{1}{2}\begin{pmatrix}\tilde{W}_x(j)\\ \tilde{W}_y(j)\end{pmatrix}.\overrightarrow{ji} \end{cases} \tag{15}$$

The limiting process are then used before performing (7) with Φ_{ij} defined as in (13) with the conservative variables obtained from (15). (See [5])

- **Implicit schemes :**

The second-order backward Euler scheme is written as follows:

$$\frac{aW^{n+1} + bW^n + cW^{n-1}}{\Delta t^n} + \frac{1}{area(i)}\sum_{j\in K(i)} \Phi^{n+1}(W_i, W_j) = 0$$

where a,b and c are well chosen parameters,

$$\alpha = \frac{\Delta t^{n-1}}{\Delta t^n} \qquad \begin{aligned} a &= \frac{\alpha+2}{\alpha+1} \\ b &= -\frac{\alpha+1}{\alpha} \\ c &= -a-b \end{aligned}$$

and α is the ratio of the old time step to the new one. The linearized delta form is given below.

$$[a\mathbb{I} + \Delta t\mathcal{A}(W^n)]\delta W^{n+1} = c(W^n - W^{n-1}) - \delta\hat{W}$$

where $\delta\hat{W}$ is the explicit flux defined by (13).
In order to achieve a really second-order implicit scheme in both space and time the linearization $\mathcal{A}$ of Φ has to be a second-order spatial approximation. Here we get the δ-scheme with explicit fluxes using the previous method for second-order accuracy in space, and solely a first-order operator $\mathcal{A}$. For investigation with a spatially second-order operator see [14].

3.5 Boundary conditions

We consider only slipping walls and apply the slip condition in a weak variational way. We note $\overrightarrow{V} = (u, v)$ the velocity and W_i the variables on the boundary.

◇ Explicit phase: By applying the slip condition $\overrightarrow{V}^n . \overrightarrow{n} = 0$ in the integral form (6) we obtain for the spatial term:

$$\int_{\partial C_i \cap \partial\Omega} \mathbf{F}(W_i^n).\overrightarrow{n}\ d\sigma = \int_{\partial C_i \cap \partial\Omega} p_i^n \begin{pmatrix} 0 \\ n_x \\ n_y \\ 0 \end{pmatrix} d\sigma$$

then

$$\Phi(W_i^n) = p_b^n \begin{pmatrix} 0 \\ \eta_1 \\ \eta_2 \\ 0 \end{pmatrix}$$

with η_1, η_2 defined as in section 3.1.

◇ Implicit phase: The previous flux function can be differentiated to obtain the following Jacobian matrix:

$$A(W_i^n, \overrightarrow{\eta}) = (\gamma - 1) \begin{pmatrix} 0 & 0 & 0 & 0 \\ \frac{(u^2+v^2)}{2}\eta_1 & -u\eta_1 & -v\eta_1 & \eta_1 \\ \frac{(u^2+v^2)}{2}\eta_2 & -u\eta_2 & -v\eta_2 & \eta_2 \\ 0 & 0 & 0 & 0 \end{pmatrix}$$

4 Numerical results

Most of the numerical results are obtained with Sod shock tube [12]. For our purpose other shock tubes will also be used ; the physical problem is briefly described in the following section. We use a 2-D code on a regular 101×3 mesh in a square tube to solve these 1-D problems.

4.1 The shock tube physical problem

A diaphragm at x_0 separates two regions which are both at rest with different thermodynamical states. Figure B shows the initial conditions with Sod's values and the evolution of the variables after the diaphragm was broken. If we consider the phenomenon at times before the waves reflected from the ends of the tube, an analytical solution can be obtained [22]. This exact solution depends only on $(x-x_0)/t$. Points (a) and (b) are the locations of the tail and the head of the simple rarefaction wave, point (c) is a contact discontinuity, it is the position reached by an element of fluid initially at x_0. The shock is located at (d) where all variables are discontinuous.

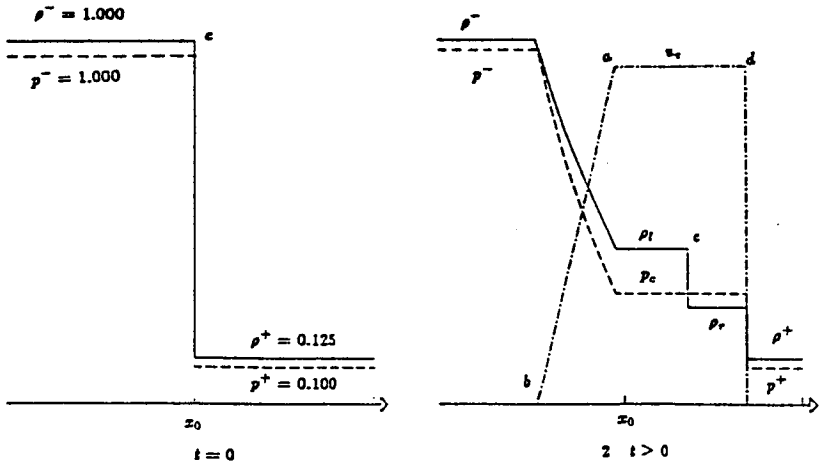

Figure B : Sod's shock tube problem

This shock tube problem is considered as the transonic case, the largest value of the Mach number ($Ma = |u|/c$) is $Ma = 0.93$, a value close to unity. The other shock tube problems we consider involve a supersonic case and a very subsonic case ; we will refer to them as the strong shock tube problem and the weak shock tube problem. The initial data and the corresponding Mach number are given below.

- Sod shock tube problem :

$$u^+ = u^- = 0.$$
$$p^+ = 1. \quad p^- = .1$$
$$\rho^+ = 1. \quad \rho^- = .125$$
$$max(Ma) = 0.93$$

- Strong shock tube problem :

$$u^+ = u^- = 0.$$
$$p^+ = 100. \quad p^- = 1.$$
$$\rho^+ = 50. \quad \rho^- = 1.$$
$$max(Ma) = 2.04$$

- Weak shock tube problem :

$$u^+ = u^- = 0.$$
$$p^+ = 1. \quad p^- = .9$$
$$\rho^+ = 1. \quad \rho^- = .8$$
$$max(Ma) = 0.039$$

4.2 Sod shock tube problem

The following notations are used to distinguish the schemes:

SW	for Steger-Warming scheme
OS	for Osher scheme
VL	for van Leer flux vector splitting
VIJ	for Vijayasundaram scheme
HVL	for van Leer flux difference splitting
ROE	for Roe scheme

4.2.1 The explicit schemes

◇ First-order results:

We can compare in figures 1 and 2 all the first-order explicit schemes. The results are shown with a CFL number ($\Delta t.max(\lambda_i)/\Delta x$) of 0.9 at time $t = 0.16$, that is to say after 46 time steps.
The 3 Q-schemes and Osher scheme give almost identical results. The Steger-Warming scheme is different from these ones essentially by the rarefaction wave

and the contact discontinuity which are extremely smeared. Moreover, an overshoot appears at the top of the velocity profile. The common point with van Leer flux vector splitting is one extra point in the shock. Van Leer scheme differs by a slight overshoot barely noticeable on the velocity profile, and the tail of the rarefaction wave which is kept as an angular point.
The Steger-Warming scheme is the most diffusive and gives poorer results, van Leer scheme leads to a slight overshoot, and the other schemes give better results on this test case. Oscillation free results are obtained but the contact dicontinuity is extremely smeared by all these schemes.

◇ Second-order results:

Figure 3 shows the results obtained with the predictor/corrector scheme. From the previous results we compare only one of the Q-scheme (Roe's one), Osher scheme and van-Leer scheme. For Roe scheme and Osher scheme with a CFL number of 0.9, 46 time steps were required to get the solution, as for the first-order computations. The contact discontinuity and rarefaction wave are better represented. For van Leer scheme, 55 time steps were required because of overshoots.
We may conclude that for this shock tube problem it is not necessary to use an elaborated scheme as Osher one. Neither the first-order scheme nor the second-order scheme give better results than those obtained with Roe schemes.

4.2.2 The implicit schemes

◇ First-order linearized schemes:

We first compare the three Q-schemes by mixing implicit and explicit phases. We use the largest CFL number (namely 18) that gives stable computation with the less robust Q-scheme (Vijayasundaram scheme). Results are shown in Figures 4 and 5, the two axes refer to the two phases in the δ-formulation. For all these schemes the contact discontinuity is barely visible from the density profile. The shock wave is extremely smeared, that is not surprising because this wave is faster than the other ones. The tail of the rarefaction wave is very sharp, this phenomenon occurs at the first time step and leads to negative pressure at the following time steps when larger CFL number are used. We can already conclude that it is better to use the same scheme for the implicit and explicit phase, except for implicit HVL- explicit ROE combination that seems to perform well. The largest CFL was obtained for Roe scheme and was only 23. By these methods, Sod shock tube problem is solved in three time steps.
Others results are shown for Steger-Warming scheme and van-Leer scheme in Figure 6. For Steger-Warming scheme the CFL number is only 14 and 18 for van-Leer

scheme. As in the previous results, the Steger-Warming scheme has the worst behavior. Van Leer scheme gives a velocity value upstream to the shock which is below the real value, and a lot of oscillations. Netherveless, we have to mention that Sod shock tube problem can be computed with this scheme in only one time step.
These implicit results allow to distinguish the Q-schemes ; Vijayasundaram scheme is the less robust one, Roe scheme the most robust and moreover, its fundamental property (8) make it the simpler one to implement. As we will see later a little correction of this scheme allows to compute this shock tube problem in one time step too and without oscillation.

◇ Non linear implicit scheme:

Results are presented in Figure 7 with a CFL number of 20 for Roe scheme. The procedure is very expensive, for each time step it requires 5 Newton iterations at less, and involves the resolution of the system. Although at the first time step the solution is much less sharp than in the other methods, the rarefaction wave remains too sharp and the CFL number cannot be increased over the previous limit. The reason is due again to the failure of Roe scheme in the rarefaction wave. At the first time step, for large CFL number Roe scheme leads to negative pressure at the second Newton iteration.

◇ Partly second-order extension:

Figure 8 represents results from M.U.S.C.L spatial second-order method, and from the temporal second-order backward Euler scheme. The two procedures are used both separately and together, as indicated in the figure. By using solely a second-order explicit phase the shock wave is better resolved than using three levels in the time discretisation. The combination of the backward Euler scheme with the M.U.S.C.L approximation in space is apparently not the right way to construct a second-order accurate implicit scheme. A phase error appears because of the three level scheme and becomes dramatic when the CFL number is increased.

4.3 The weak and strong shock tube problems

From previous results we clonclude that Steger-Warming scheme is not adapted to our purpose (to choice an accurate and robust scheme). The explicit and implicit schemes built from this flux function give the poorest results. Osher explicit scheme is very expensive and we did not build the implicit scheme. Roe scheme is the most robust scheme of the Q-schemes family. Van Leer scheme has the surprising property to compute Sod shock tube problem with arbitrarily large CFL

flow calculations. We make this choice using the criteria of stability, robustness, accuracy and computational cost.

Sod shock tube problem:

We recall that all the explicit first-order schemes behave well in that transonic case (oscillation free results are obtained) but they are not accurate enough in the contact discontinuity. Steger-Warming scheme gives the poorer results. Osher scheme is the most elaborate scheme we use but it gives results quite like the results obtained with a Q-scheme or van Leer flux vector splitting.
Their second-order extension in space and time leads to rather good results, the contact discontinuity is better resolved.

The first-order implicit linearized schemes have been compared with large CFL numbers. We did not build the linearized implicit Osher scheme because the explicit Osher scheme is the most expensive of the explicit schemes. The largest CFL numbers that give stable computations are the following:

Schemes	Steger-Warming	Van Leer	Q	Corrected Q
CFL numbers	14	∞	18 to 23	∞

The lower and upper bounds for the Q-schemes are given respectively by Vijayasundaram scheme and Roe scheme. Steger-Warming scheme does not behave well, it is not robust and stable enough and it is very diffusive. Van leer can compute this test in one time step but it is less accurate than a Q-scheme and very diffusive too. This last characteristic is important, because the diffusion is an essential parameter in the dynamics of flames or for Navier-Stokes equations. Q-scheme can fail in rarefaction waves, but Harten's corrective procedure circumvents this without noticeable additional CPU time.
The second-order extension is not yet efficient and is currently improved, but with solely spatial second-order in the explicit phase, the results are rather good and the procedure is very cheap.
We have tested a non-linear method combined with Roe scheme. The procedure is not more efficient than the implicit linearized and does not allow to use larger CFL number, but we used false Jacobian. Although this non-linear algorithm is too much expensive it is interesting to note it can be used to get a second-order formulation in both space and time. It would be also interesting to test the non-linear algorithm with the differentiable van Leer flux vector splitting but it would remains too expensive.

From the previous results we have renounced to use Steger-Warming scheme.

Among the Q-scheme, Vijayasundaram scheme and Roe scheme can be written in a simpler form than van Leer Q-scheme, which is an advantage for computational cost. Roe scheme is also the most robust scheme of the Q-scheme family. We pursue the comparisons with only Roe scheme and van Leer flux vector splitting and the implicit linearized formulation.

Strong and weak shock tube problems:

The strong shock problem does not lead to note-worthy differences between the two schemes. The rarefaction wave is partly mistaken with a shock by the two schemes which involve a limited CFL number for stable computations.

the subsonic case is the most useful for our purpose. Clearly it reveals that van Leer scheme is less accurate and also less robust than a Q-scheme for low Mach number flows. The CFL condition is more restrictive for van Leer explicit scheme than for Roe explicit scheme. Moreover, Roe implicit scheme can be used with larger CFL number than van Leer implicit scheme. The results obtained with identical CFL number are quite better for Roe scheme which can compute the weak shock tube problem in one time step without any correction.

The choice of a flux function clearly depends on the problem to solve. Four our purpose Roe scheme seems to be a good candidate.
The choice of the formulation to get accurate solutions is not straightforward. For computational cost reasons we have no option but to use the implicit linearized δ-formulation. Modifications such as partly implicit formulations can be thought to get a cheap and accurate formulation.

ACKNOWLEDGEMENTS

The author is indebted to L. Fezoui who has supervised this study and gave the numerical results for Osher, van Leer and Steger-Warming schemes, and to A. Dervieux for his fruitful advices.

References

[1] S. R. CHAKRAVARTHY, K. Y. SZEMA, "An Euler Solver for Three-Dimensional Supersonic Flows with Subsonic Pockets", AIAA JULY 16-18, (1985).

[2] A. DERVIEUX, "Steady Euler Simulations Using Unstructured Meshes", VKI Lecture Series, (1985).

[3] J.A. DESIDERI, E. HETTENA, "Numerical Simulation of Hypersonic Equilibrium-Air Reactive Flow", INRIA report Aout 1987.

[4] G. FERNANDEZ, H. GUILLARD, "An Implicit Method for the Computation of Reactive Flows", Accepted to 12th IMACS WORLD CONGRESS, July 1988.

[5] F. FEZOUI, "Résolution des équations d'Euler par un schéma de van Leer en éléments finis", INRIA Report n^o 358, 1985.

[6] L. FEZOUI, B. STOUFFLET, "A class of implicit upwind schemes for Euler simulation with unstructured meshes", to appear in J.C.P.

[7] L. FEZOUI H. STEVE, "Décomposition d'un flux Van-Leer pour résoudre les équations d'Euler en éléments finis", INRIA report Sophia Antipolis, to appear.

[8] A. HARTEN, "High Resolution Schemes for Hyperbolic Conservation Laws", Supplemented Mathematical Subject Classification 65P05 , 35 L65, 76L05, 1980.

[9] A. HARTEN, P.D. LAX, B. VAN LEER, "On upstream Differencing and Godunov-type Schemes for Hyperbolic Conservation Laws", ICASE Report 82-5, 1982.

[10] S. OSHER, F. SOLOMON, " Upwind difference schemes for hyperbolic systems of conservation laws", J. Math. Computation , 1982.

[11] P. L. ROE, "Approximate Riemann solvers, parameter vectors anddifference schemes", J. Comp. Phys., 43, p. 357, 1981.

[12] G. A. SOD, "A survey of Several Finite Difference Methods for Systems of Nonlinear Hyperbolic Conservation Laws", J. Comp. Phys. 27, (1977).

[13] J. STEGER, R.F. WARMING,
" Flux vector splitting for the inviscid gas dynamic with applications to finite difference methods", J.C.P., 40 pp 263-293, 1981.

[14] H. STEVE, "Schémas implicites linéarisés décentrés pour la résolution des équations d'Euler en plusieurs dimensions", Thesis, to appear (1988).

[15] B. STOUFFLET, "Résolution numérique des équations d'Euler des fluides parfaits compressibles par des schémas implicites en éléments finis", Thesis, Univ. of Paris, 1984.

[16] B. VAN LEER, "Computational methods for ideal compressible-flow", Von Karman Institute For Fluid Dynamics, Lectures series , 1983.

[17] B. VAN LEER, "Towards the ultimate conservative difference scheme I. The quest of monotonicity",Lecture notes in Physics, Vol. 18 page 163, 1972.

[18] B. VAN LEER, "On the relation between the upwind-differencing schemes of Godunov, Engquist-Osher and Roe", ICASE Report n^o 81-11, (1981).

[19] B. VAN LEER, "Flux Vector Splitting for the Euler equations", Lecture Notes in Physics, vol. 170. page 405-512, 1982.

[20] G. VIJAYASUNDARAM, "Transonic flow simulations using an upstream-centered scheme of Godunov in Finite-Element",J. Comp. Phys. 63, (1986).

[21] R. F. WARMING, R. M. BEAM, "On the construction and application of implicit factored schemes for conservation laws", SIAM AMS Proceedings,Volume 11, (1978).

[22] G. B. WHITHAM, "Linear and nonlinear waves", Wiley, New-York, (1974).

Sod shock tube

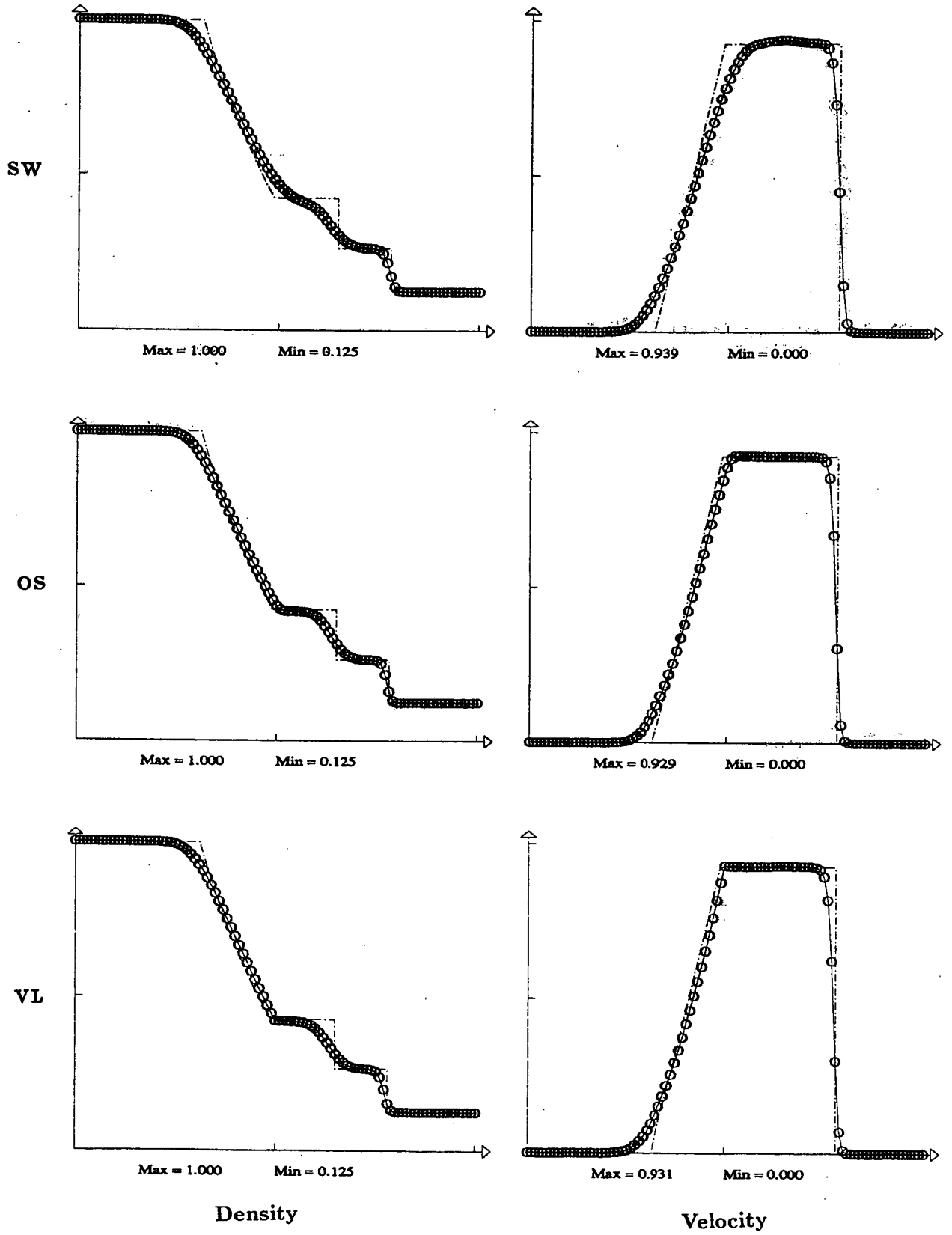

t=0.16 CFL=0.9 46 time steps

Fig 1 : First-order explicit schemes

Sod shock tube

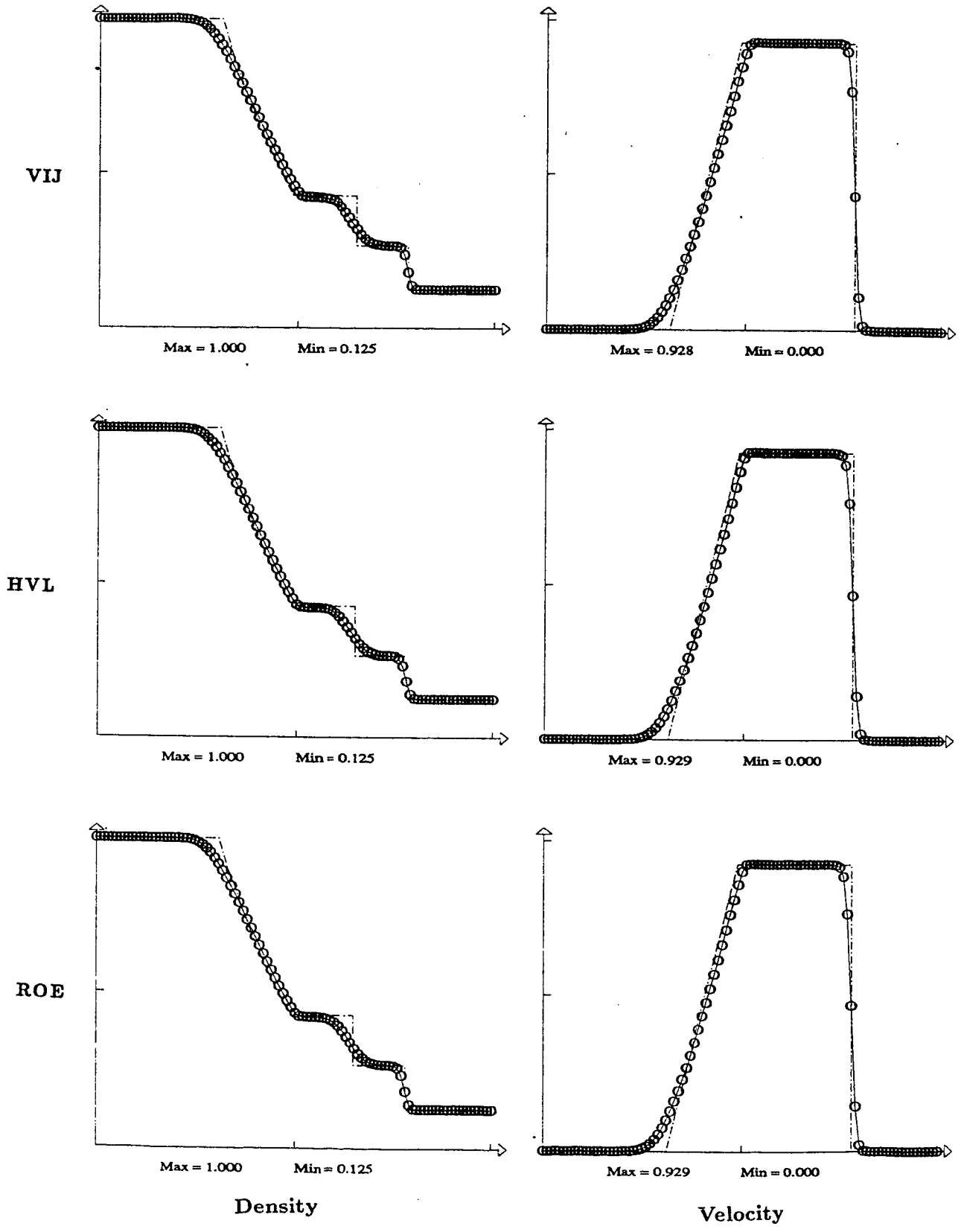

t=0.16 CFL=0.9 46 time steps

Fig 2 : First-order explicit schemes

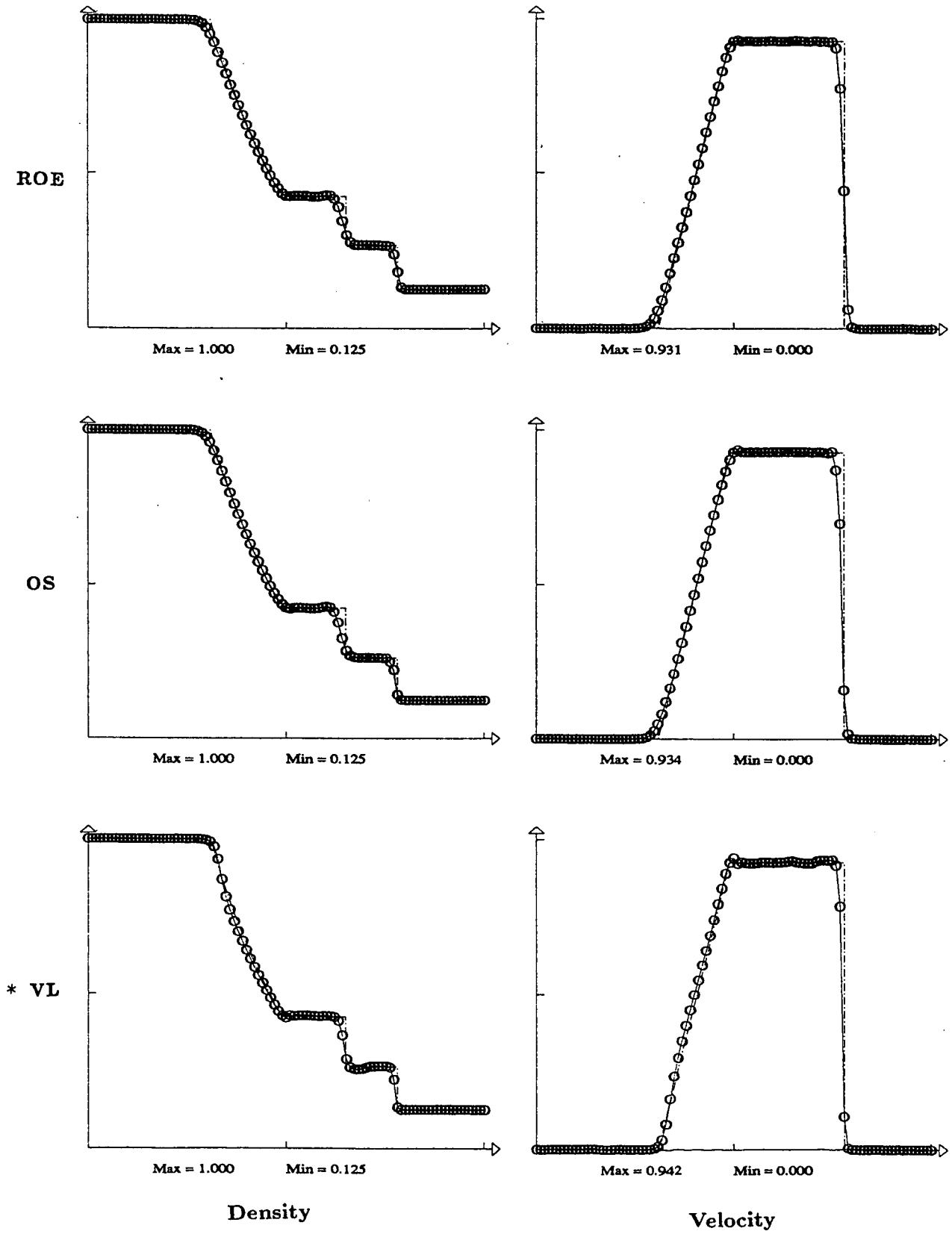

t=0.16 CFL=0.9 46 time steps * 55 time steps

Fig 3 : Second-order explicit schemes

Sod shock tube

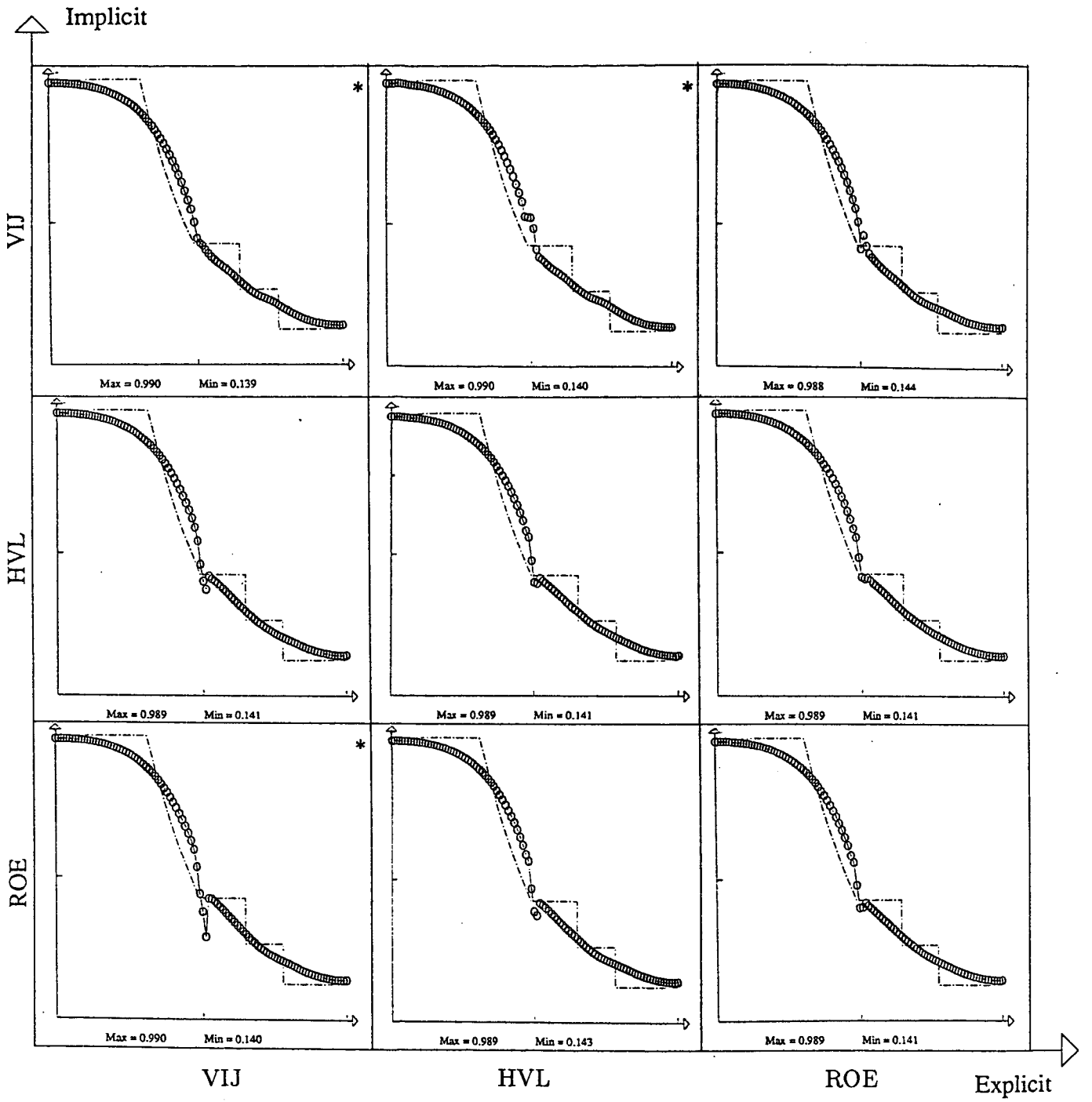

CFL = 18
Time = 0.16
CFL = 18
Grid : 101 x 3
3 time steps
* 4 time steps

Fig 4 : First-order linearized Q-schemes (density)

Sod shock tube

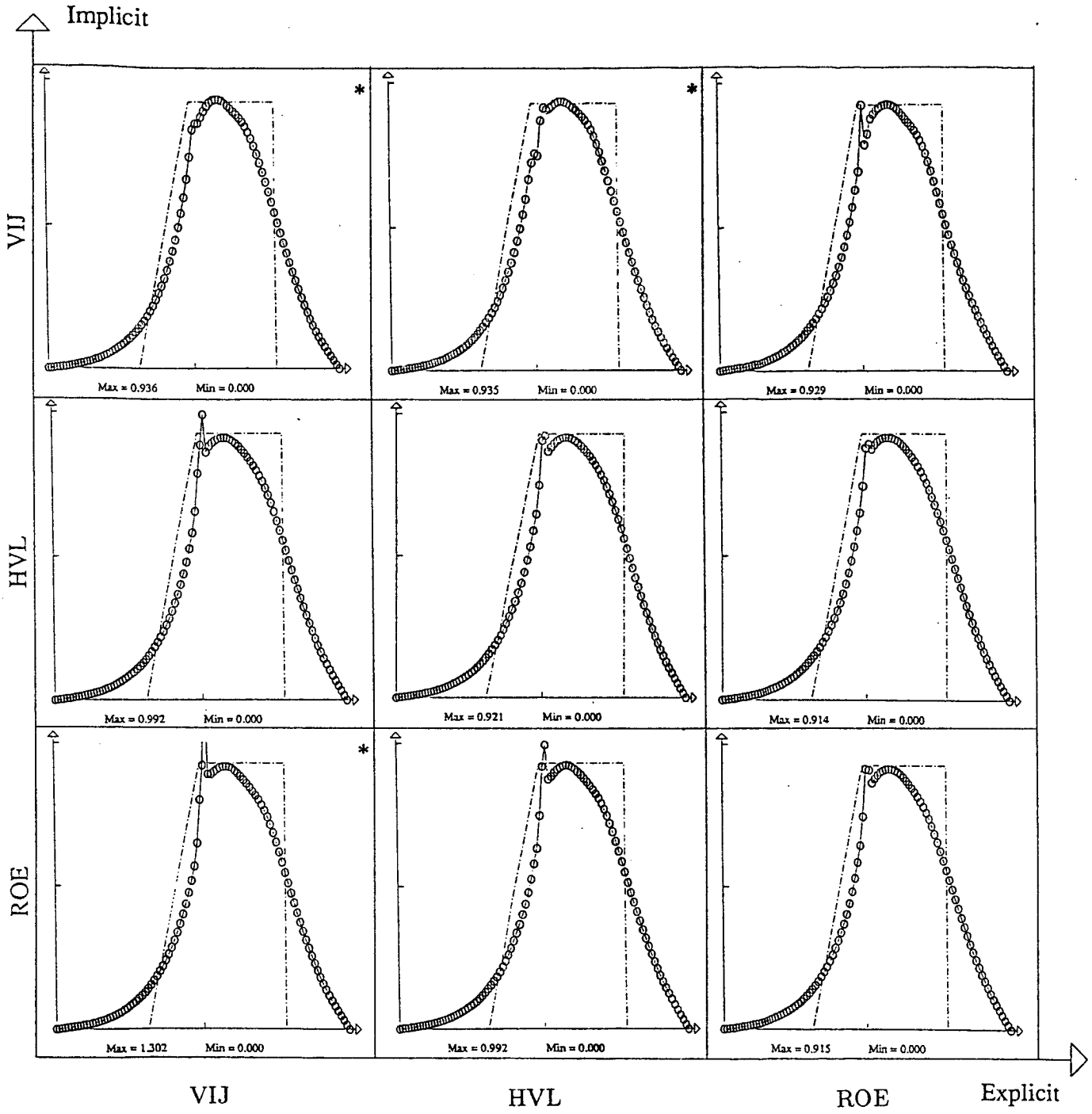

CFL = 18
Time = 0.16
CFL = 18
Grid : 101 x 3
3 time steps
* 4 time steps

Fig 5 : First-order linearized Q-schemes (velocity)

Sod shock tube

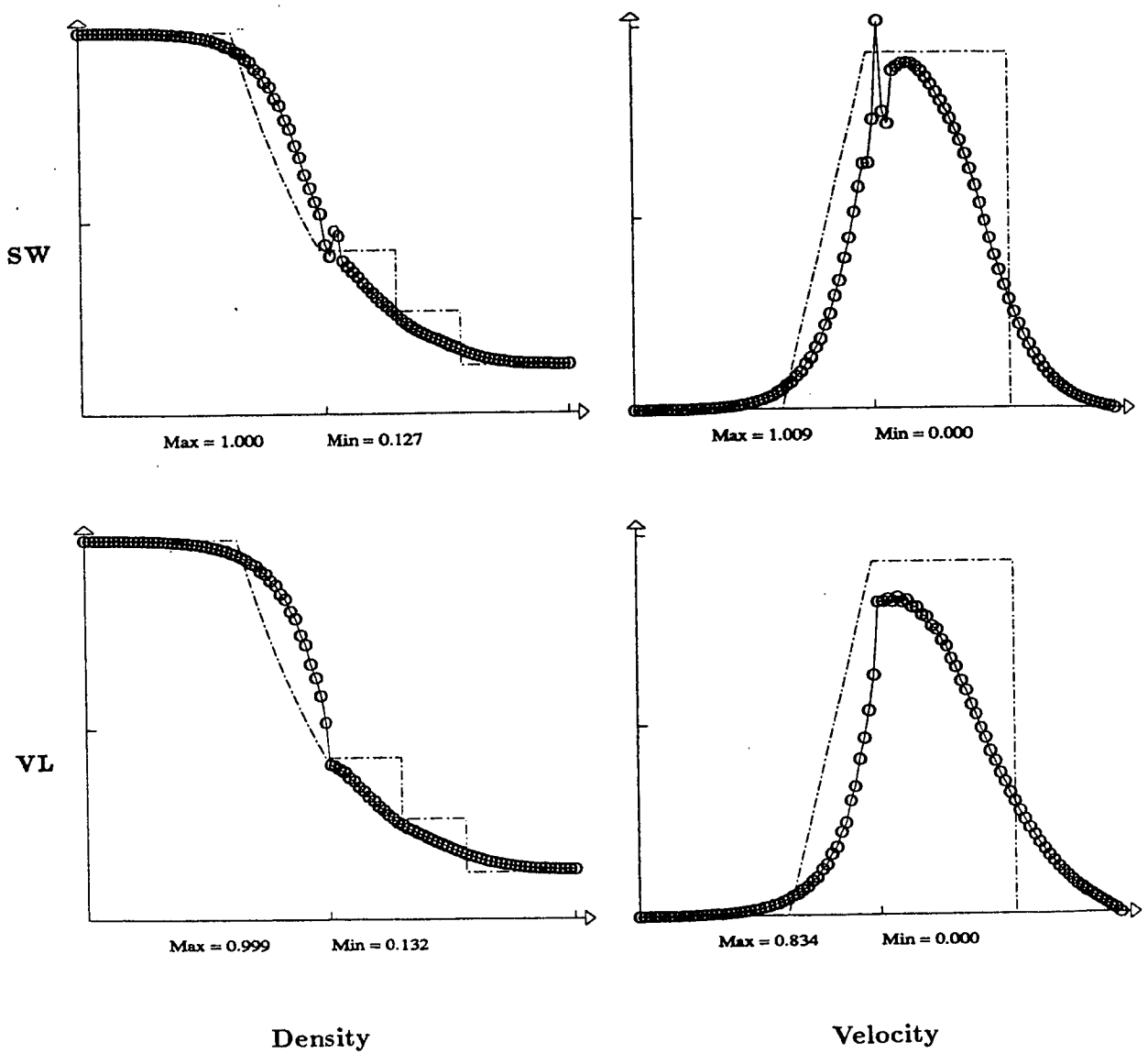

VL : t=0.16 CFL=18 3 time steps

SW : t=0.16 CFL=14 5 time steps

Fig 6 : First-order linearized schemes

Sod shock tube

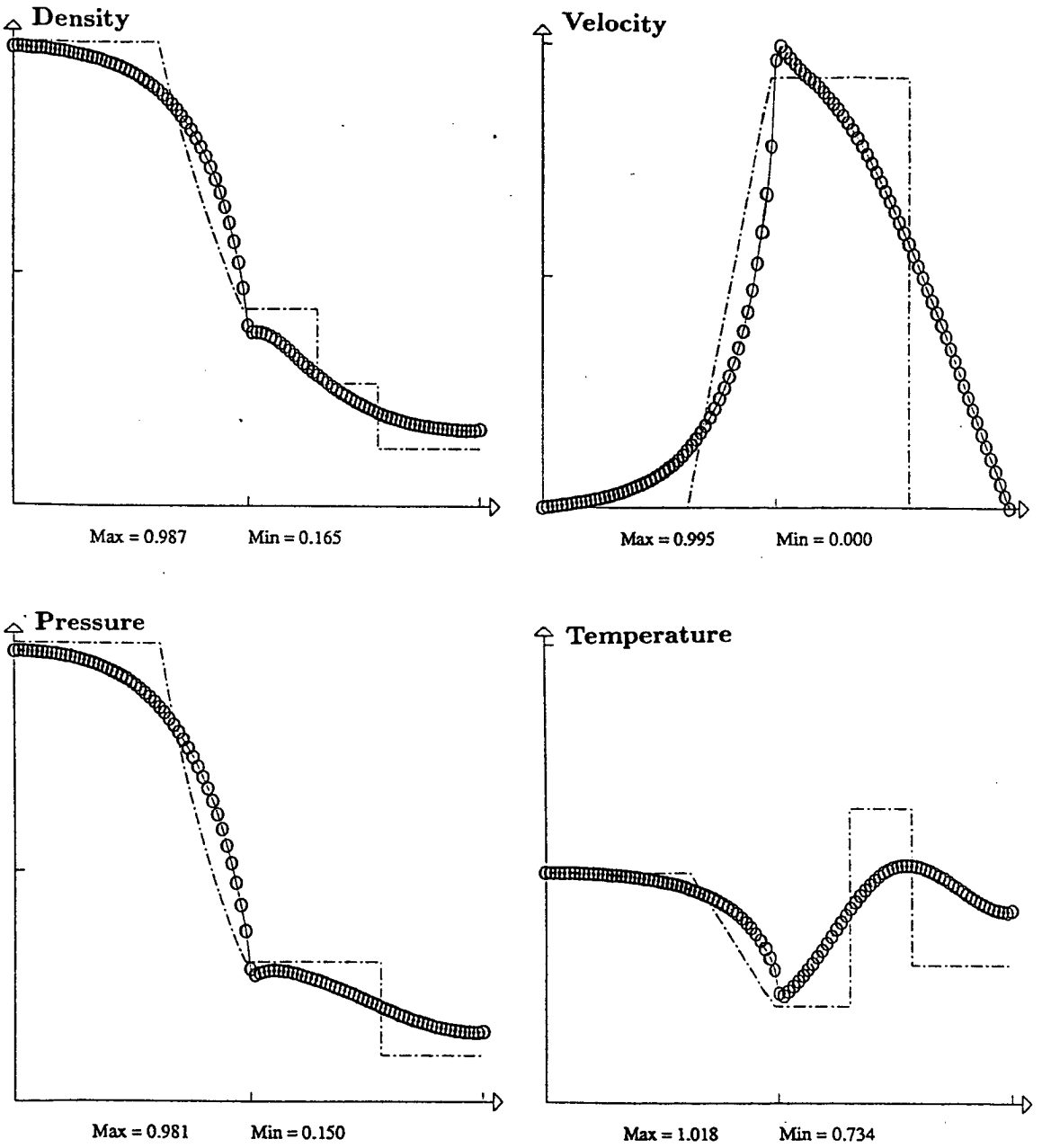

t=0.16 CFL=20 3 time steps

Fig 7 : Non linear implicit Roe scheme

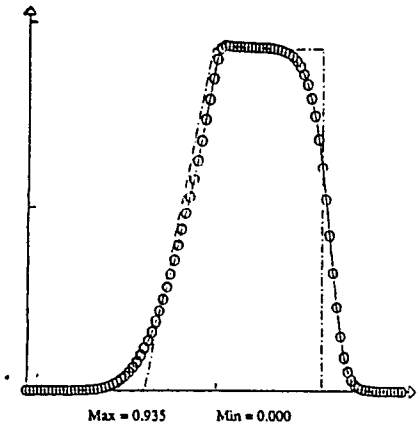

$(O(\Delta t), O(\Delta x), O(\Delta x))$

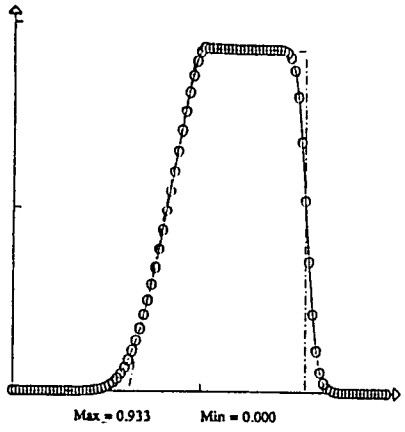

$(O(\Delta t), O(\Delta x), O(\Delta x^2))$

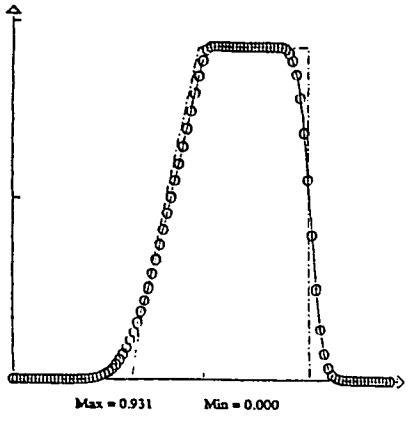

$(O(\Delta t^2), O(\Delta x), O(\Delta x))$

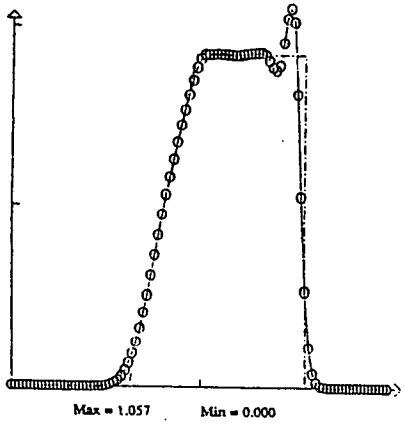

$(O(\Delta t^2), O(\Delta x), O(\Delta x^2))$

Implicit Roe : CFL=1 38 time steps

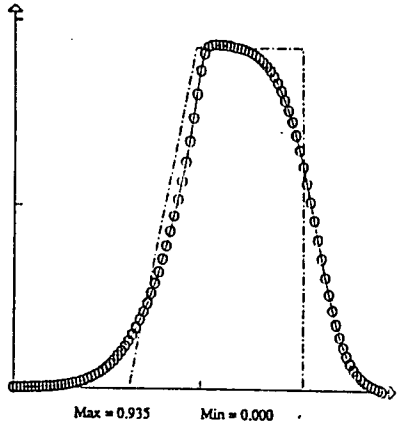

$(O(\Delta t), O(\Delta x), O(\Delta x))$

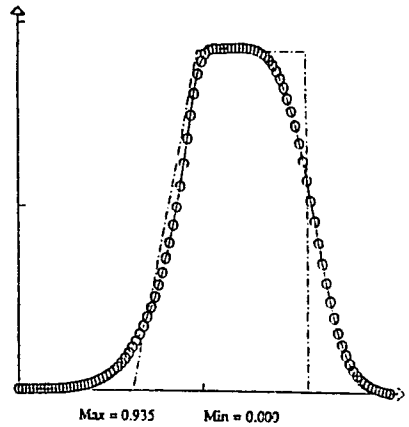

$(O(\Delta t), O(\Delta x), O(\Delta x^2))$

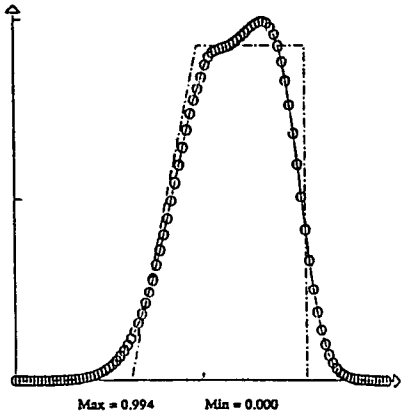

$(O(\Delta t^2), O(\Delta x), O(\Delta x))$

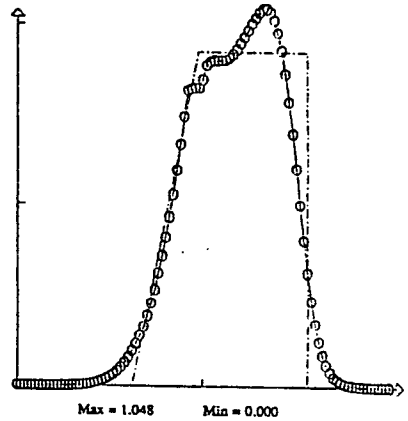

$(O(\Delta t^2), O(\Delta x), O(\Delta x^2))$

Implicit Roe : CFL=5 8 time steps

Fig 8 : Second-Order extensions of Roe scheme (Velocity)

legend:(a,b,c) a accuracy in time
b spatial accuracy for implicit phase
c spatial accuracy for explicit phase

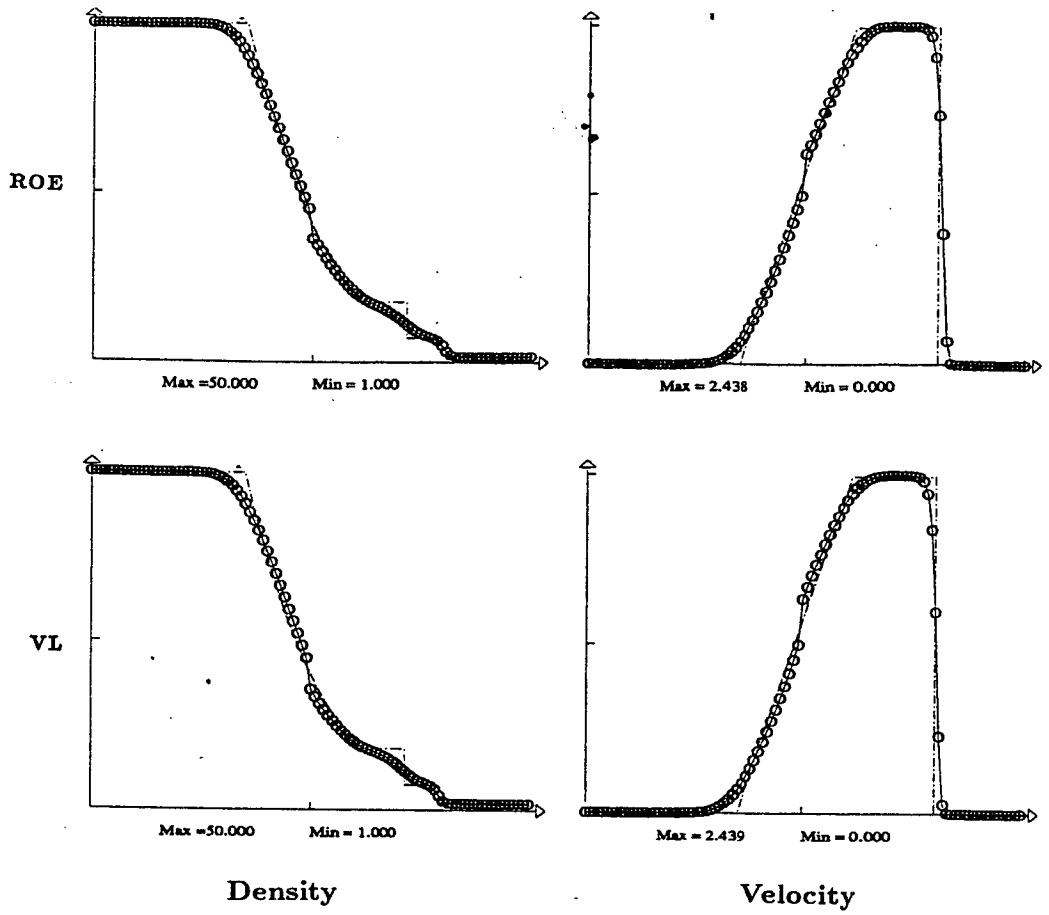

a/ Explicit schemes: CFL=0.9

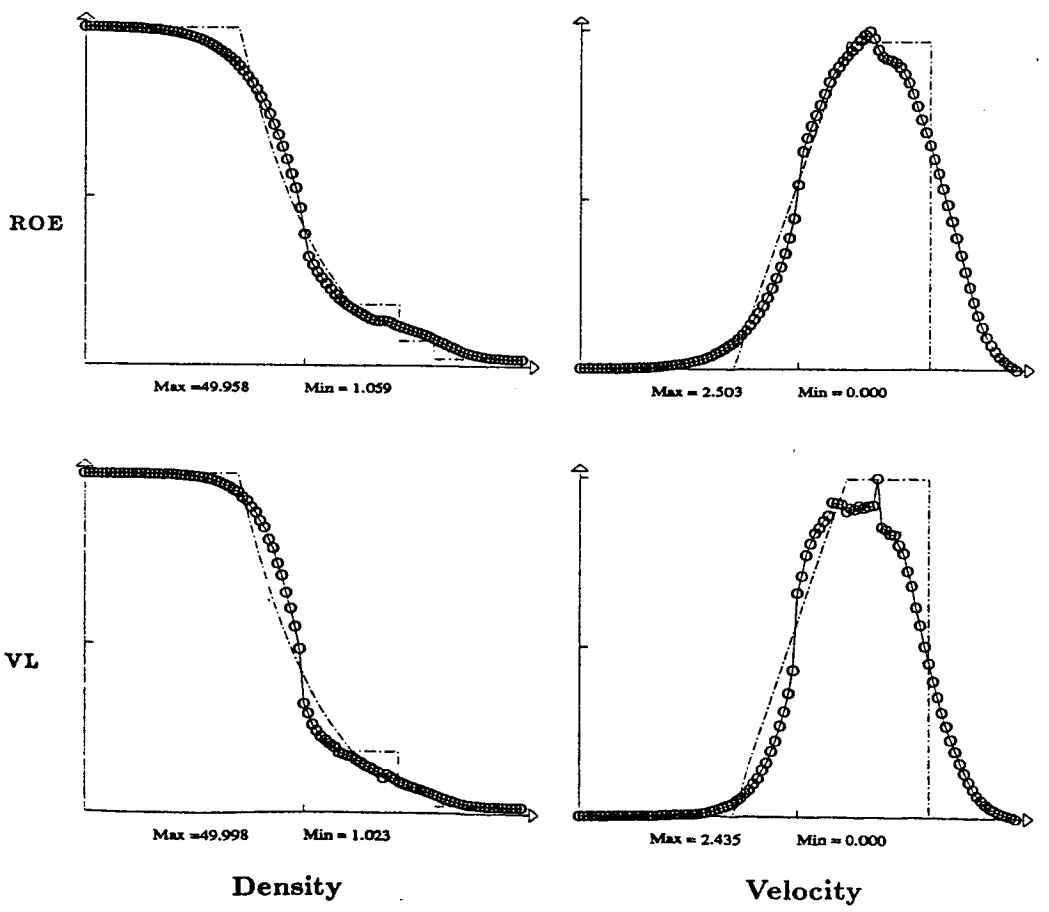

b/ Implicit schemes: CFL=11

Fig 9 : Strong shock tube problem t=0.09

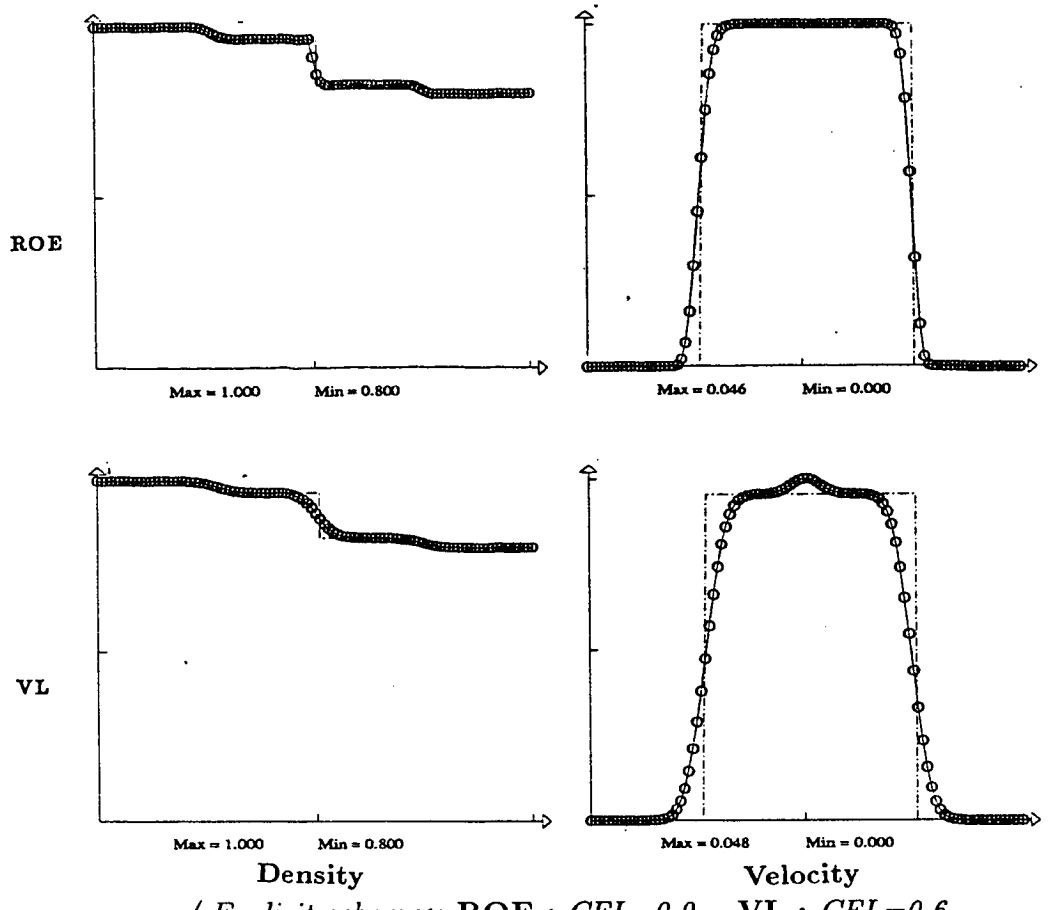

a/ Explicit schemes: **ROE** : *CFL=0.9* **VL** : *CFL=0.6*

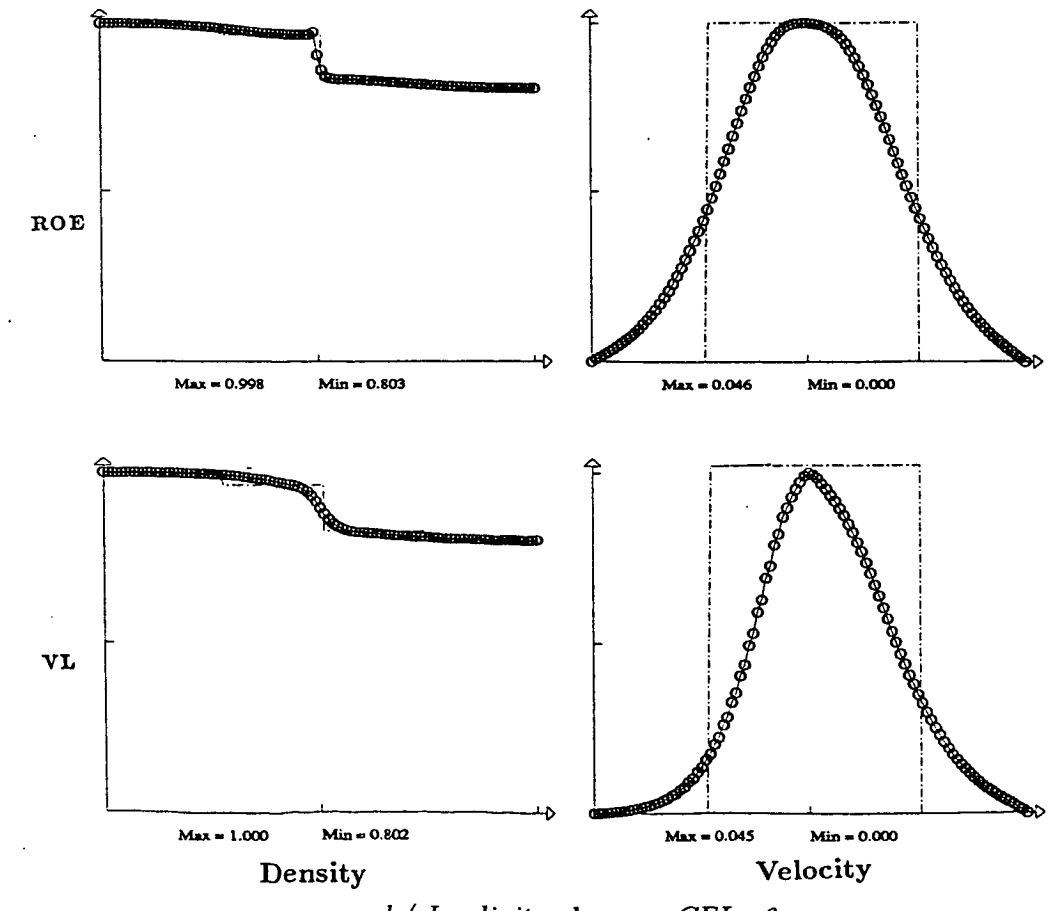

b/ Implicit schemes: CFL=6

Fig 10 : Weak shock tube problem t=0.20

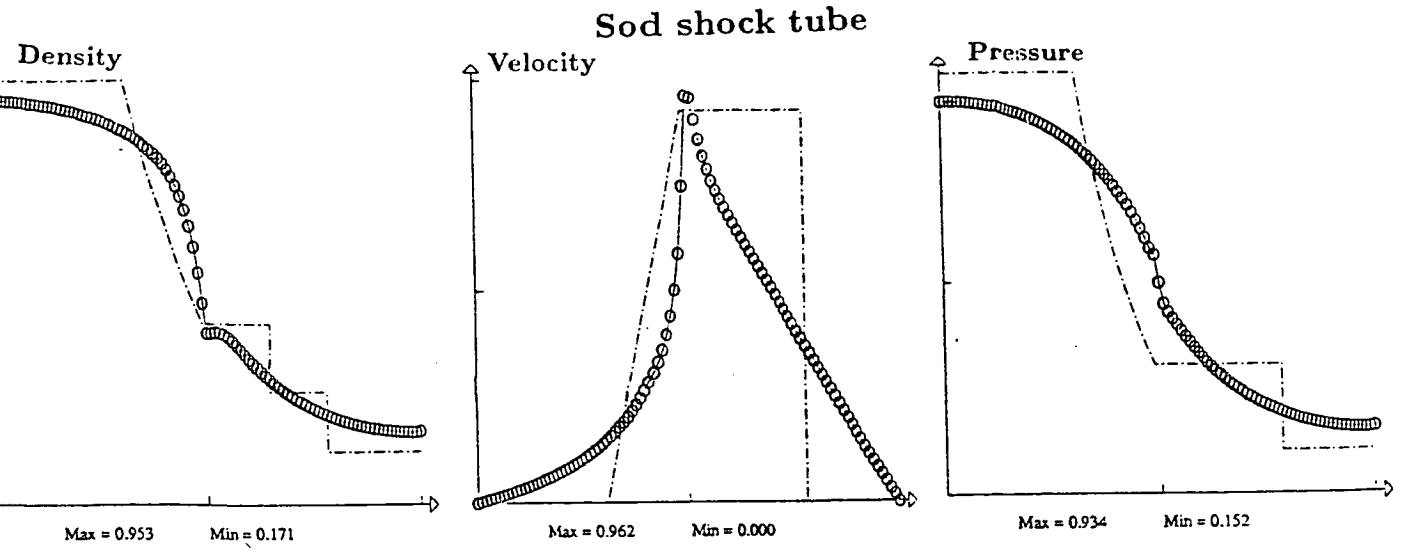

a : *t=0.16* *1 time step* $\epsilon = 0.5$

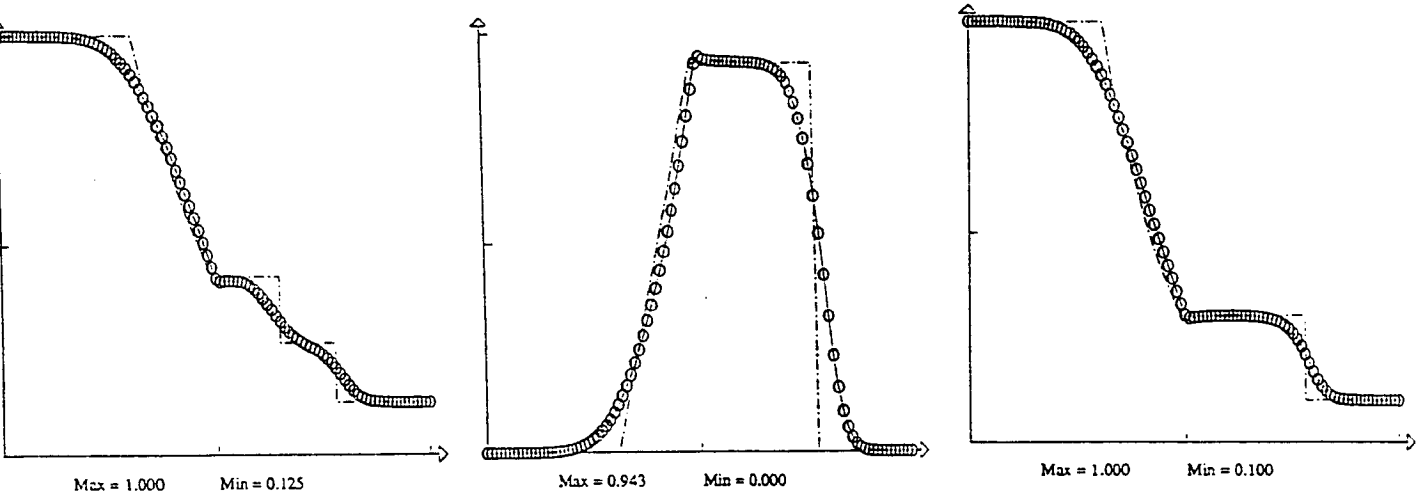

b : *t=0.16* *37 time steps* $\epsilon = 0$

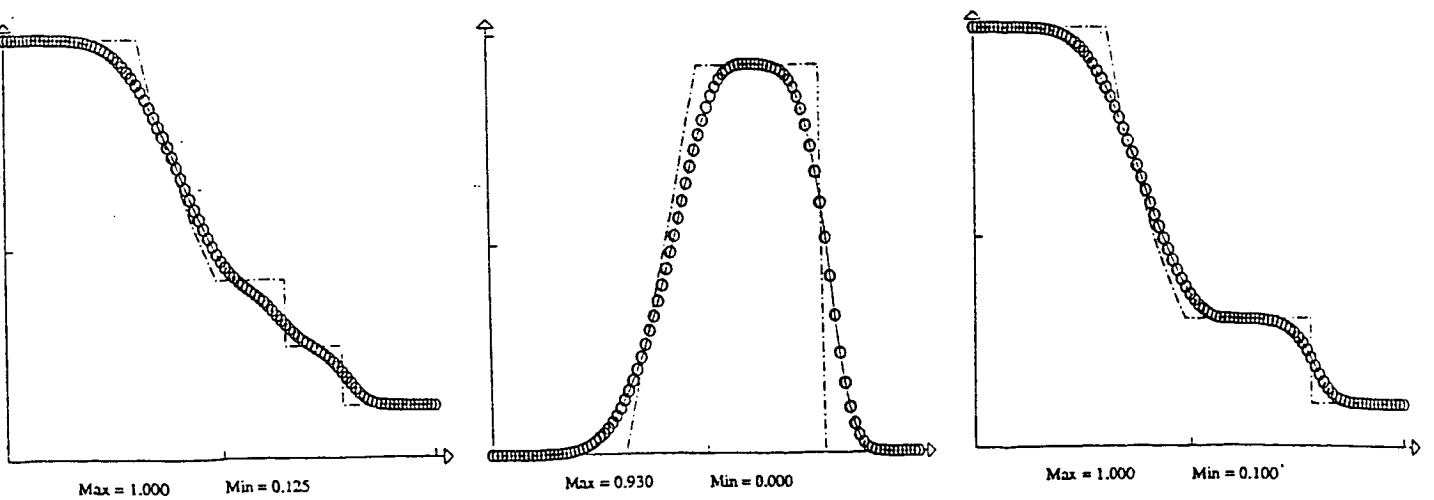

c : *t=0.16* *36 time steps* $\epsilon = 0.5$

Fig 11 : Harten's correction of the Q-scheme

SHOCK TUBE

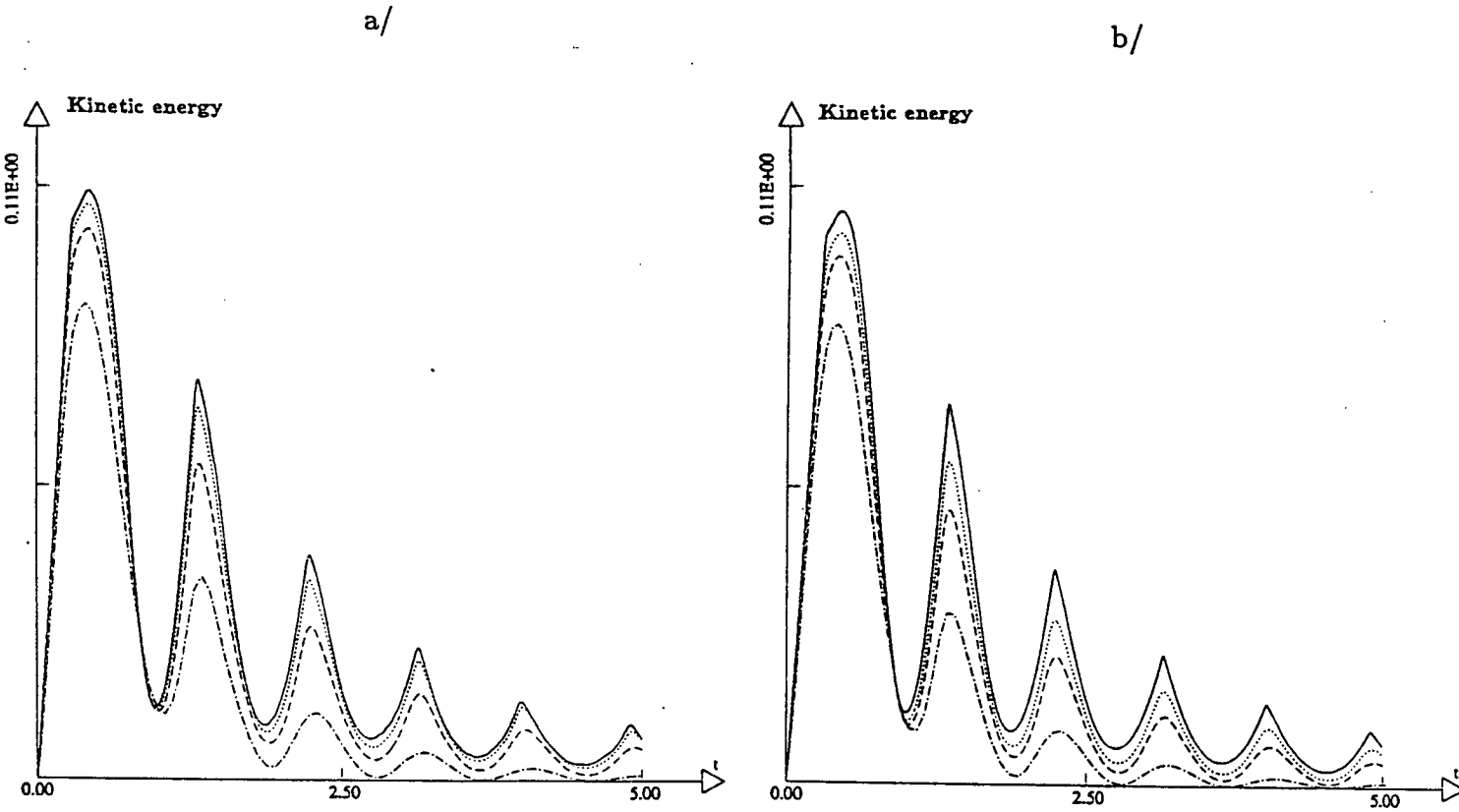

——— Explicit CFL = 1

····· Implicit CFL = 1

- - - - - - Implicit CFL = 3

-·-·-·- Implicit CFL = 10

Fig 12 : Dissipation for Roe's Q-scheme

Imprimé en France
par
l'Institut National de Recherche en Informatique et en Automatique